

Brief communication (Original)

Multimodal imaging fiducial markers for kinematic measurement of joint models

Jae Won You^a, Yeon Soo Lee^b, Hong Moon Sohn^a^aDepartment of Orthopaedic Surgery, Chosun University Hospital, ^bDepartment of Biomedical Engineering, Catholic University of Daegu, Gyungbuk 712-702, Republic of Korea

Background: Fiducial markers are objects placed in the field of view of an imaging system for use as a point of reference or a measure. There is no information regarding suitable markers for joint models.

Objectives: We compared the fiducial markers commonly used in X-ray, CT, and MRI imaging modalities.

Methods: The markers tested were plastic balls, ceramic balls, passive reflective balls, liquid-filled balls, and steel balls. The balls were scanned using X-ray, CT, and MRI systems. The scanned X-ray images were reviewed if it the markers are able to be expressed. The tomographic images of CT and MRI were converted into 3D ball models and then the reconstructed shapes and dimensions of the balls were examined. The dimensional accuracy of expression and reconstruction was calculated in terms of the mean and the standard deviation.

Results: There was no marker that can be expressed in all the imaging modalities. Alternatively, we propose a synthetic marker that is composed of a hard sphere and a fat tissue wrapping. The hard ball is for X-ray and CT imaging, while the fat tissue is for MRI imaging.

Conclusion: A synthetic marker composed of a hard sphere and a fat tissue wrapping can a multimodal fiducial marker.

Keywords: Accuracy, fiducial marker, multimodal, registration

The spatial landmark, i.e. fiducial marker, is a necessary tracking tool for clinical as well as research applications. Various kinds of fiducial markers have been used for clinical applications such as navigation assisted surgeries in the orthopedic, prostate, brain, and facial bone treatments, and marker-based multimodal fusion in the PET-CT diagnosis. A set of gold markers (Civico medical solutions, Orange city, IA, USA) was used to indicate the prostate cancer region for radiotherapy [4]. Titanium screws in the mastoid region were used for accuracy evaluation of skin-surface contour based navigation assisted temporal bone surgery [8]. Glass beads with a diameter of 4 mm were used for multimodal registration of simulated phantoms having various degrees of renal artery stenosis as phantoms [11].

Research applications of fiducial markers include accuracy evaluation in multimodal 3D/3D image fusion or 2D/3D image fusion for measuring the internal body joint kinematics of living humans, animals, or cadavers.

In the accuracy tests of in vivo joint kinematics measurement utilizing 2D/3D image registration, fiducial markers should be detectable on both X-ray and CT images without artifact. The 3D/2D image registration fits the posture of a 3D bone model to a 2D X-ray image by numerically minimizing the discrepancy in gradient and/or silhouette between a 2D X-ray images and a virtual 2D X-ray images digitally created from a 3D model [6, 13]. The 3D bone models are reconstructed from CT or MRI images, while the 2D target images are normal X-ray images [13, 15, 16]. The accuracy validation of in vivo joint kinematics using 3D/2D image registration can be quantified by comparing controlled and measured 3D translations or rotations of fiducial markers [19].

For the consideration of soft tissue constraints such as ligament or capsules in the joint kinematics, a 3D joint model including soft tissues and hard bones is strongly required. This kind of musculoskeletal joint model can be built by combining CT- and MRI-derived 3D models, so called 3D/3D image registration [14]. As in the accuracy evaluation of the 3D/2D image registration, the accuracy of 3D/3D image registration is evaluated by using rigid fiducial markers [14].

Even though there have been many demands for multimodal fiducial markers as mentioned above, it is not easy to find a commercially available multimodal fiducial marker widely applicable to musculoskeletal kinematics studies. Hence, most researchers have to use custom-built fiducial markers. The current study aims to report and suggest fiducial markers that can be expressed commonly in X-ray, CT, and MRI imaging modalities, especially for application in orthopedic joint kinematic studies.

Materials and methods

Fiducial markers

Five types of ball markers were prepared as listed in **Table 1**. Even though initially a stainless ball, i.e., the femoral head component, was included in the X-ray and CT imaging tests, it was excluded at the MRI imaging test because it has severe metal artifact as a result of differences in magnetic susceptibility in clinical MRI [12]. All of the markers were sphere shaped and had diameters of 8–11.6 mm.

The plastic ball was a plastic bead for a necklace and had a hole in it for passing of a necklace string to connect the beads. The ceramic ball was made of zirconia. The navigation ball was a reflective fiducial marker used for tracking of joint alignment during Ortho Pilot navigation assisted orthopedic surgery (Aesculap, Center Valley, Pa, USA). The navigation ball was a plastic sphere coated with a reflective material, i.e., ScotchLite 8010 (3M, USA), and had a hole to allow it to be mounted on a tracking frame.

The CT-marker and MRI-marker are skin markers used as landmarks during gamma knife neurosurgery for brain tumors, and register an intraoperative skull to a preplanned surgical model.

The CT-marker for neurosurgery is for CT scanning of the brain, while the MRI-marker was for MRI scanning. The CT-marker is a sphere, which can be settled in a concave plastic base, while the MRI-marker is a spherical soft plastic shell whose inside was filled with water. The water in the MRI-marker creates a powerful magnet signal because unpaired protons in each water molecule have been aligned in a large magnetic field [9].

X-ray scanning

X-ray images were taken of all the markers. The X-ray images were taken using a distortion free digital X-ray scanner (GE, USA). The resolution of the X-ray images was higher than 1900×2991 in a 24 bit JPEG. A digital X-ray scanner was chosen because digital X-ray devices have negligible pin-cushion distortion compared with fluoroscope X-ray scanners.

To compare imaging detectability of fiducial markers, with respect to soft and bone tissues, fiducial markers were mounted onto a porcine femur. The navigation ball markers were mounted using a 2-stage bolt-nut system, composed of two plastic bolts of 3.5 mm in diameter and one nut (**Figure 1**) [14]. Plastic balls were fixed onto the porcine femur using a wood stick (**Figure 2**). The ceramic ball, CT-marker, and MRI-marker were fixed onto a concave home that was machined for settlement of fiducial markers. In our preliminary tests, a plastic panel of thickness 2 mm showed a radio transmittance similar to the medium-thickness soft tissue of the human fingers (**Table 1**). For this reason, the plastic panel was placed under the markers when taking CT X-ray images to simulate the occlusion effect of soft tissue.

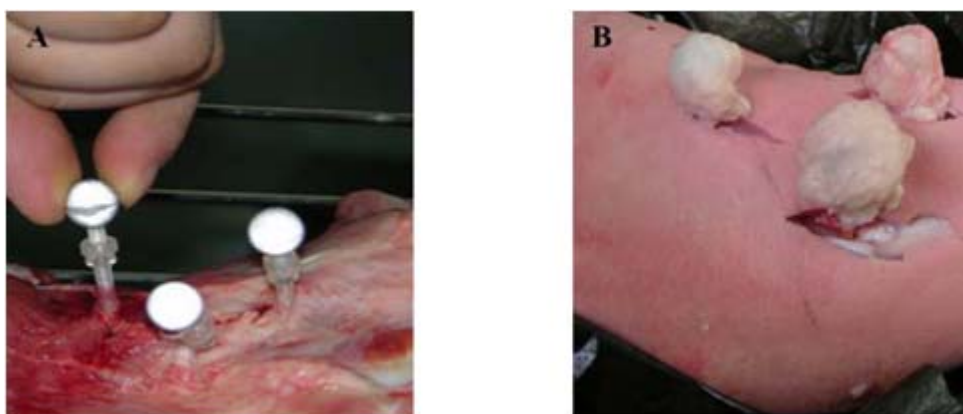


Figure 1. Mounting and encapsulation of the navigation ball markers for MRI scanning. **A:** Navigation ball markers were mounted at the screw end of the two-step plastic screw system that is fixed to a porcine bone. **B:** subsequently, the navigation ball markers were encapsulated with subcutaneous fat for MRI scanning.

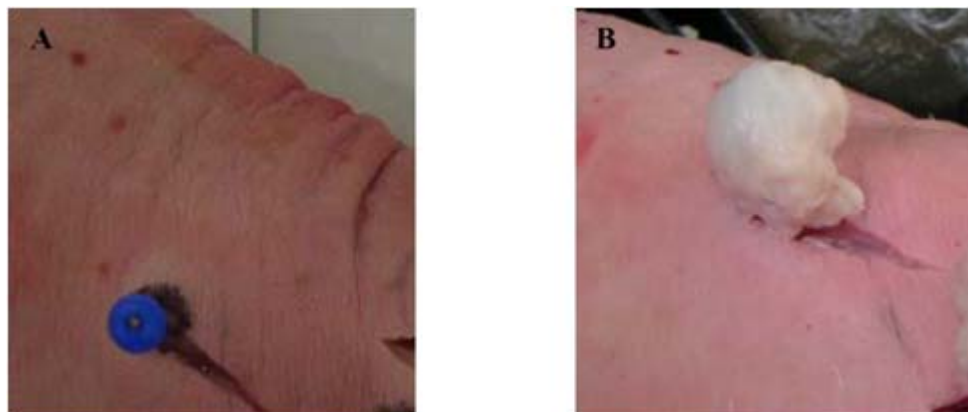







Figure 2. Mounting and encapsulation of the plastic ball markers for MRI scanning. **A:** Each of three plastic balls is mounted at the end of a wood stick that is fixed to a porcine bone. **B:** subsequently, the plastic ball marker was encapsulated with subcutaneous fat for MRI scanning.

Table 1. Fiducial markers tested

Marker	Diameter (mm)	Picture	Manufacturer or provider
Plastic ball	8		Top Jewelry Factory, Hejiang, China
Ceramic (Alumina)	10.4		Shinil Ceramics, Gwangju, Korea
Navigation ball	11.6		Passive navigation marker used in the OrthoPilot navigation surgery system Aesculap, Center Valley, Pa, USA.
CT-marker (Brain Lab)	8		CT skin marker made of plastic, fixed in a concave shape plastic housing (BrainLab, Germany)
MRI-marker (Brain Lab)	8		MRI skin marker whose inside is filled with a liquid, fixed in a concave shape plastic housing (BrainLab, Germany)

CT and MRI scanning

The ball markers were scanned using a 16-channel CT (GE, USA) and using an MRI Signa Excite 1.5 T system (GE, USA). CT scanning was performed with 1.25 mm slice thickness and a 0.625 mm reconstruction interval. MRI scanning was done with 1.20 mm slice

thickness using fat suppression FIESTA sequence. FOVs of CT and MRI scanning were approximately 230 mm × 230 mm and 200 mm × 200 mm, respectively. The transverse resolutions of CT images and MRI images were approximately 0.3 mm × 0.3 mm and 0.4 mm × 0.4 mm, respectively.

For MRI scanning, 4 fiducial markers without hydrogen, i.e., the plastic ball, ceramic ball, navigation ball, and CT-marker, were encapsulated with subcutaneous fat that was harvested from fresh porcine thigh. Because those markers do not have unpaired protons like hydrogen molecules, they do not induce magnetism [9]. The porcine fat is composed of carbon 76.54%, hydrogen 11.94%, and oxygen 11.52% and can be magnetized in the MRI scanning [2]. Hence, the nonaqueous fiducial markers encapsulated with porcine fat can be detected in MRI imaging.

Reconstruction of CT-derived and MRI-derived 3D models

CT-derived and MRI-derived 3D models of the ball markers and the porcine femur were reconstructed using Mimics software, version 13.1 (Materialise, Leuven, Belgium). The CT-derived bone model was constructed based on the image contour with a threshold over 250 Hounsfield Units (HU). Bone contour was manually extracted from the MRI images and MRI-derived 3D bone and marker models were reconstructed.

Detectability index

The detectability of each fiducial marker was quantified using a custom scoring system. Detectability of a fiducial marker was qualitatively scored by 5 credit levels; 5 for very excellent, 4 for excellent, 3 for moderate, 2 for marginal, and 1 for poor.

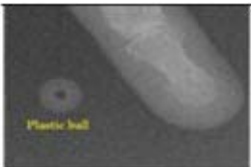


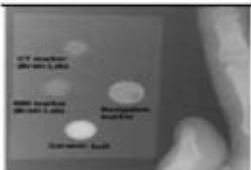
In the evaluation scoring system, judgement of score can be subjective. Hence, the most important score judgement is ‘moderate = 3’ representing the marker’s feasibility for the imaging modality. The score equal to or higher than ‘moderate’ score was given only when the boundary of the image is clearly shown and there is no interobserver disagreement.

Results

X-ray images (Table 2)

The plastic ball showed a comparable gray level to soft tissue of the phalanges. Its signal became less distinguishable when it is placed on the plastic panel, because of similar X-ray transmittance (T2b). Despite the occlusion effect of the plastic panel, the ceramic ball is shown very clearly (T2b and d). The navigation ball was fairly distinguishable despite the occlusion effect of the plastic panel. The CT-marker and MRI-marker showed weak intensity similar to the plastic ball (T2d).

Table 2. X-ray images of the fiducial markers

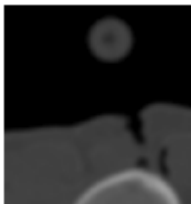
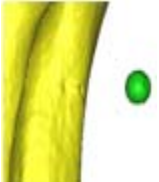


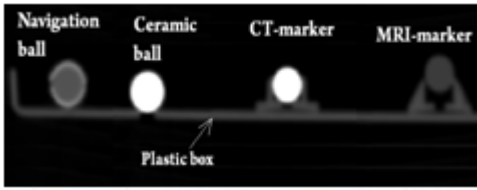
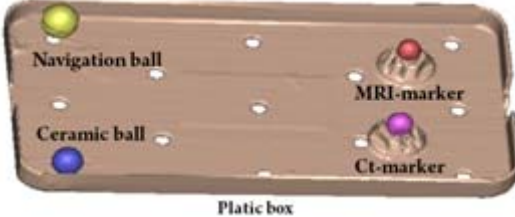
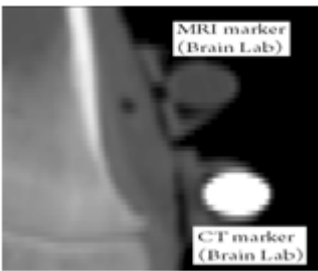
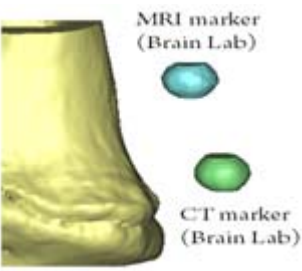
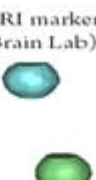
Marker	Diameter (mm)	Camera image	X-ray image
Plastic ball	8	N/A	 (T2a)
Ceramic (Alumina)	10.4	 (T2c)	 (T2b)
Navigation ball	11.6		 (T2d)
CT-marker (Brain Lab)	8		
MRI-marker (Brain Lab)	8		

CT images and CT-derived 3D models (Table 3)

In CT images, the plastic ball showed a similar gray level to soft tissue of the phalanges as in the X-ray images (T3a). In contrast, the ceramic ball and CT-marker were clearly distinguishable from one another (T3c and e). The ceramic ball signal was quite strong compared with soft tissue or cortical bone (T3-c). The outer shell of the navigation ball was expressed slightly stronger than plastic box (T3-f). The CT-marker showed a fairly distinguishable

intensity, while the MRI-marker's intensity was similar or poorer than the plastic ball or soft tissue (T3f, g, and a). With the CT images where the markers were overlapping or contacted plastic material or living tissue, the 3D models of the ceramic ball, navigation ball, and CT-marker were able to be reconstructed automatically or semi-automatically without manual segmentation, while the plastic and MRI-maker could not be reconstructed without manual segmentation.

Table 3. The CT images and CT-derived models of the fiducial markers

Marker	Diameter (mm)	CT image	3D model reconstructed
Plastic ball	8	 (T3a)	 (T3b)
Ceramic (Alumina)	10.4	 (T3c)	 (T3d)
Navigation ball	11.6	 (T3e)  (T3f)	
CT-marker (Brain Lab)	8	 (T3g)	 (T3h)
MRI-marker (Brain Lab)	8		

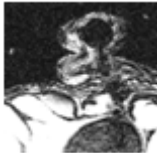

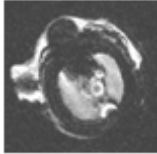
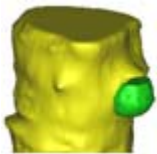

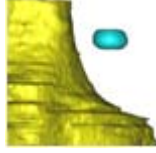
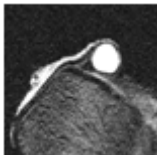

MRI images and MRI-derived 3D models (Table 4)

In MRI imaging, the plastic ball, ceramic ball, and navigation ball were distinguishable because they are enclosed by porcine fat possessing hydrogen atoms (T4a, c, and e). Even though the MRI image of the CT-marker is not demonstrated, it was able to be shown when enclosed by the porcine fat, in our preliminary tests. By contrast, the MRI-marker expressed itself clearly because it includes water (T4g). In reconstructing 3D models from MRI images, all the markers required manual segmentation in assigning their boundaries to neighboring living tissues, while the MRI-marker was able to be converted to a 3D model using semiautomatic and manual segmentation.

Detectability score

The detectability of fiducial makers in X-ray imaging was 5 for the ceramic ball, 4 for the navigation ball, and 2 for the remainder. The detectability in CT imaging was 5 for the ceramic ball, 4 for the brain-marker, and 2 for the remainder. The detectability in MRI imaging was scored 4 because the MRI-marker can express itself by reactively making a material specific-magnet field because of its water content, but its flexible spherical surface was slightly deformed when subjected to compression derived from the tension of neighboring soft tissue (T4g). The other markers were able to be expressed passively only with envelopment of aqueous material and their detectability scores in MRI imaging were given as 2.

Table 4. The MRI images and MRI-derived models of the fiducial markers

Marker	Diameter (mm)	Tomograph	3D model reconstructed
Plastic ball	8	 (T4a)	 (T4b)
Ceramic (alumina)	10.4	 (T4c)	 (T4d)
Navigation ball	11.6	 (T4e)	 (T4f)
CT-marker (BrainLab)	8	N/A	N/A
MRI-marker (BrainLab)	8	 (T4g)	 (T4h)

Discussion

The current study aimed to report and suggests fiducial markers that can be expressed commonly in X-ray, CT, and MRI imaging modalities. The ceramic ball is considered the best fiducial marker for X-ray and CT imaging. The ceramic ball and other balls can be expressed by encapsulation them with fat. The MRI-marker (BrainLab, USA) whose inside is filled water can be expressed well in MRI imaging, but not in X-ray and CT imaging.

There have been many attempts to develop multimodal fiducial markers available for two or more of X-ray, CT, MRI, and even ultrasound imaging modalities. Several different sets of modality specific fiducial markers were simultaneously used for the accuracy validation of intermodality 2D/3D image registration for the in vivo joint kinematics [7, 18]. Two caps installed on a bone fiducial screw were used for multimodal imaging. One of the two caps was made of metal for CT imaging, while another was made of plastic whose inside is filled with diluted saline [1]. An invasive angiography catheter filled with gadolinium DTPA (an MRI contrast agent) and fat was also used as fiducial marker for X-ray, CT, MRI, electroportal imaging device, and computed radiographic imaging [10]. The use of 18K Au/Cu alloy fiducial markers embedded into hydrated tissue was proposed for CT-MRI image fusion purposes [17].

The ceramic ball is considered a good multimodal fiducial marker resulting in no artifact for X-ray, CT, and MRI imaging. For the MRI scanning, of course, the ceramic ball has to be encapsulated with aqueous material. In terms of radio transmittance, the ceramic is comparable to pearl, but without pearl artifact on CT or MR images [21].

The MRI-marker (BrainLab, USA) has a problem in that it deforms easily from external loads. The deformation of the spherical shape will yield wrong geometrical information and will yield wrong location information as landmarks for the accuracy check of multimodal image registration.

Hence, a fiducial ball marker combining a hard ceramic shell and MR contrast material will be the best multimodal fiducial marker. There have been several types of multimodal fiducial makers combining CT contrast material and MRI contrast material. The cylindrical fiducial marker made of a Plexiglas outer diameter of 8 mm, a length of 12 mm and a refillable cavity with a volume of 21.25 mm³. For MRI, the markers are filled with water containing special

chemicals for CT, T1, and T2 MRI, and SPECT examinations [20]. Another fiducial marker was fabricated from polymethylmethacrylate (Lucite/Perspex) and incorporated a cylindrical cavity with 6

l of fluid containing 80 kBq^{99mTc} mixed with gadodiamide MR contrast medium. The fiducial markers were used to check the error of SPECT to MR coregistration [3]. Fiducial markers by mimicking tissue material (agar gel with antibacterial) surrounding the vessel have been fabricated and were detectable in all modalities without distortion [5]. However, the multimodal fiducial markers reported in the literature including MR contrast were cylindrical and were made for guiding a surgeon's hand to the location of disease parts. The spatial recognition of a cylindrical marker can be dependent on the direction of the CT or MRI scanning axis. However, the tomographic images of spherical markers will not be dependent on the scanning axis because of the 3D spatial symmetry of the sphere. Therefore, the authors propose a fiducial marker that has a spherical outer shell made of zirconia (ZrO₂), alumina (Al₂O₃), or pearl (CaCO₃) and is filled with aqueous material inside the shell.

Conclusions

A ceramic ball was evaluated the best fiducial marker for X-ray and CT imaging. A ceramic ball and other balls can be expressed in MRI by encapsulating them with fat. The authors of the current study propose a fiducial marker that has a spherical outer shell made of zirconia (ZrO₂), alumina (Al₂O₃), or pearl (CaCO₃) and is filled with aqueous material inside the shell.

Acknowledgement

This work was supported by grants from the Clinical Medicine Research Institute of Chosun University Hospital (2013). The authors declare no conflict of interest.

References

1. Ammirati M, Gross JD, Ammirati G, Dugan S. Compariosn of registration accuracy of skin- and bone-implanted fiducials for frameless stereotaxis of the brain: a prospective study. *Skul Base*. 2002; 12: 125-30.
2. Armsby HP. *The principles of animal nutrition*. J. Wiley and Sons, New York; 1908.
3. Barnden L, Kwiatek R, Lau Y, Hutton B, Thurfjell L, Pile K, et al. Validation of fully automatic brain SPET to MR co-registration. *Eur J Nucl Med*. 2000; 27:

- 147-54.
4. Choi Y, Ahn SH, Lee HS, Hur WJ, Yoon JH, Kim TH, et al. Clinical usefulness of implanted fiducial markers for hypofractionated radiotherapy of prostate cancer. J Korean Soc Ther Radiol Oncol. 2011; 29:91-8.
5. Cloutier G, Soulez G, Quanadli SD, Allard L, Qin Z, Cloutier F, et al. A multimodality vascular imaging phantom with fiducial markers visible in DSA, CTA, MRI, and ultrasound. Med Phys. 2004; 31:1424-33.
6. Dennis DA, Komistek RD, and Mahfouz MR. In vivo fluoroscopic analysis of fixed-bearing total knee replacements. Clin Orthop Relat Res. 2003; 410:114-30.
7. Gendrin C, Markelj P, Pawiro SA, Spoerk J, Bloch C, Weber C, et al. Validation for 2D/3D registration I: The comparison of intensity- and gradient-based merit functions using a new gold standard data set. Med Phys. 2011; 38:1491-502.
8. Grayeli AB, Esquia-Medina G, Nguyen Y, Mazalaigue S, Vellin J-F, Lombard B, et al. Use of anatomical or invasive markers in association with skin surface registration in image-guided surgery of the temporal bone. Acta Oto-Laryngologica. 2009; 129:405-10.
9. Hendee WR, and Morgan CJ. Magnetic resonance imaging. Part I—physical principles. West J Med. 1984; 141:491-500.
10. Ho JU, Chen MF, Chen WC. The feasibility study of customized fiducial markers in image fusion and position markers for radiation therapy. Proceedings of Korean Radio Therapist Association Conference. 2008; 43:99-100.
11. King DM, Fagan AJ, Moran CM, Browne JE. Comparative imaging study in ultrasound, MRI, CT, and DSA using a multimodality renal artery phantom. Med Phys. 2011; 38:565-73.
12. Kolind SH, Mackay AL, Munk PL, Xiang QS. Quantitative evaluation of metal artifact reduction techniques. J Magn Reson Imaging. 2004; 20:487-95.
13. Komistek RD, Dennis DA, Mahfouz M. In vivo fluoroscopic analysis of the normal human knee. Clin Orthop Relat Res. 2003; 410:69-81.
14. Lee YS, Seon JK, Shin VI, Kim GH, Jeon M. Anatomical evaluation of CT-MRI combined femoral model. Biomed Eng Online. 2008; 7:6.
15. Li G, Defrate LE, Rubash HE, Gill TJ. In vivo kinematics of the ACL during weight-bearing knee flexion. J Orthop Res. 2005; 23:340-4.
16. Li G, Wuerz TH, Defrate LE. Feasibility of using orthogonal fluoroscopic images to measure in vivo joint kinematics. J Biomech Eng. 2004; 126:314-8.
17. Parker CC, Damyanovich A, Haycocks T, Haider M, Bayley A, Catton CN. Magnetic resonance imaging in the radiation treatment planning of localized prostate cancer using intra-prostatic fiducial markers for computed tomography co-registration. Radiother Oncol. 2003; 66:217-24.
18. Pawiro SA, Markelj P, Pernus F, Gendrin C, Figl M, Weber C, et al. Validation for 2D/3D registration I: A new gold standard data set. Med Phys. 2011; 38: 1481-90.
19. Takao M, Nishii T, Sakai T, Sugano N. Application of a CT-3D fluoroscopy matching navigation system to the pelvic and femoral regions. Comput Aided Surg. 2012; 17:69-76.
20. Vikhoff-Baaz B, Bergh AC, Starck G, Ekholm S, Wikkelso C. A new set of fiducial markers for MRI, CT and SPET alignment. Nucl Med Commun. 1997; 18:1148-54.
21. West JJ, Patel AR, Kramer CM, Helms AS, Olson ES, Rangavajhala V, et al. Dynamic registration of preablation imaging with a catheter geometry to guide ablation in a Swine model: validation of image integration and assessment of catheter navigation accuracy. J Cardiovasc Electrophysiol. 2010; 21:81-7.